

Original Article  
Microbiology



# Potential of polylactic-co-glycolic acid (PLGA) for delivery Jembrana disease DNA vaccine Model (pEGFP-C1-tat)

Lalu Unsunidhal <sup>1,2</sup>, Raden Wasito <sup>3</sup>, Erif Maha Nugraha Setyawan <sup>1</sup>,  
Ziana Warsani <sup>4</sup>, Asmarani Kusumawati <sup>1,3,\*</sup>

<sup>1</sup>Department of Reproduction and Obstetrics, Faculty of Veterinary Medicine, University Gadjah Mada, Yogyakarta 55281, Indonesia

<sup>2</sup>Biomedical Field, Nursing Study Program, STIKES Yarsi Mataram, West Nusa Tenggara 83361, Indonesia

<sup>3</sup>Department of Pathology, Faculty of Veterinary Medicine, University Gadjah Mada, Yogyakarta 55281, Indonesia

<sup>4</sup>Research Center of Biotechnology, University Gadjah Mada, Yogyakarta 55281, Indonesia

 OPEN ACCESS

Received: May 5, 2021

Revised: Jul 26, 2021

Accepted: Aug 3, 2021

Published online: Aug 30, 2021

\*Corresponding author:

Asmarani Kusumawati

Department of Reproduction and Obstetrics,  
Faculty of Veterinary Medicine, University  
Gadjah Mada, Jl. Fauna No.2, Karangmalang,  
Yogyakarta 55281, Indonesia.

E-mail: uma\_vet@ugm.ac.id

Parts of the contents of this article were presented in the 1st International Conference of Advanced Veterinary Science and Technologies for Sustainable Development (ICAVESS, 28-29 March 2021) organized by the Faculty of Veterinary Medicine Gadjah Mada University, Indonesia.

© 2021 The Korean Society of Veterinary Science

This is an Open Access article distributed under the terms of the Creative Commons Attribution Non-Commercial License (<https://creativecommons.org/licenses/by-nc/4.0>) which permits unrestricted non-commercial use, distribution, and reproduction in any medium, provided the original work is properly cited.

## ABSTRACT

**Background:** The development of a vaccine for Jembrana disease is needed to prevent losses in Indonesia's Bali cattle industry. A DNA vaccine model (pEGFP-C1-tat) that requires a functional delivery system will be developed. Polylactic-co-glycolic acid (PLGA) may have potential as a delivery system for the vaccine model.

**Objectives:** This study aims to evaluate the *in vitro* potential of PLGA as a delivery system for pEGFP-C1-tat.

**Methods:** Consensus and codon optimization for the tat gene was completed using a bioinformatic method, and the product was inserted into a pEGFP-C1 vector. Cloning of the pEGFP-C1-tat was successfully performed, and polymerase chain reaction (PCR) and restriction analysis confirmed DNA isolation. PLGA-pEGFP-C1-tat solutions were prepared for encapsulated formulation testing, physicochemical characterization, stability testing with DNase I, and cytotoxicity testing. The PLGA-pEGFP-C1-tat solutions were transfected in HeLa cells, and gene expression was observed by fluorescent microscopy and real-time PCR.

**Results:** The successful acquisition of transformant bacteria was confirmed by PCR. The PLGA:DNA:polyvinyl alcohol ratio formulation with optimal encapsulation was 4%:0.5%:2%, physicochemical characterization of PLGA revealed a polydispersity index value of 0.246, a particle size of 925 nm, and a zeta potential value of -2.31 mV. PLGA succeeded in protecting pEGFP-C1-tat from enzymatic degradation, and the percentage viability from the cytotoxicity test of PLGA-pEGFP-C1-tat was 98.03%. The PLGA-pEGFP-C1-tat demonstrated luminescence of the EGFP-tat fusion protein and mRNA transcription was detected.

**Conclusions:** PLGA has good potential as a delivery system for pEGFP-C1-tat.

**Keywords:** Jembrana disease; tat gene; DNA vaccine; delivery system; PLGA

## INTRODUCTION

Bali cattle are considered one of Indonesia's superior livestock types. However, the Bali cattle's main weakness is their susceptibility to Jembrana disease [1], which is caused by the Jembrana disease virus (JDV) [2]. Economic losses caused by Jembrana disease are significant, taking the form of death of 5,000 Bali cattle in one year in the first JDV outbreak

**ORCID iDs**

Lalu Unsunnidhal   
<https://orcid.org/0000-0002-0874-6590>  
 Raden Wasito   
<https://orcid.org/0000-0002-7454-6618>  
 Erif Maha Nugraha Setyawan   
<https://orcid.org/0000-0003-0920-7086>  
 Ziana Warsani   
<https://orcid.org/0000-0002-6630-5953>  
 Asmarani Kusumawati   
<https://orcid.org/0000-0001-9828-4969>

**Funding**

This research was supported by the Direktorat Riset dan Pengabdian Masyarakat and Lembaga Pengelolaan Dana Pendidikan Republik Indonesia (LPDP RI).

**Conflict of Interest**

The authors declare no conflicts of interest.

**Author Contributions**

Conceptualization: Unsunnidhal L, Kusumawati A; Data Curation: Unsunnidhal L, Warsani Z; Formal analysis: Unsunnidhal L, Warsani Z, Kusumawati A; Funding acquisition: Kusumawati A, Wasito R, Nugraha Setyawan EM; Investigation: Unsunnidhal L, Kusumawati A; Methodology: Unsunnidhal L, Wasito R, Nugraha Setyawan EM, Warsani Z, Kusumawati A; Project administration: Unsunnidhal L, Kusumawati A; Resources: Unsunnidhal L, Warsani Z, Kusumawati A; Supervision: Wasito R, Nugraha Setyawan EM, Kusumawati A; Validation: Wasito R, Nugraha Setyawan EM, Kusumawati A; Visualization: Unsunnidhal L, Warsani Z, Kusumawati A; Writing - original draft: Unsunnidhal L, Kusumawati A.

in Indonesia and affecting the distribution of Bali cattle between islands [3]. The virus has similarities to the human immunodeficiency virus (HIV) and causes acute disease in infected cattle within a short incubation period, replicating in blood at very high titer levels and causing death within 1–2 weeks [3]. In addition, the Bali cattle death rate caused by JDV is about 17%, thus making Jembrana disease the main concern of the Bali cattle industry [3,4].

The Indonesia government has made efforts to prevent the Jembrana disease through vaccination with less than 70% protection. The vaccine has been considered less effective in preventing the spread of the Jembrana virus [5], encouraging researchers to develop DNA-based vaccines. The most important difference between DNA vaccines and other types of vaccines, which only trigger a humoral immune response, is that DNA vaccines also trigger a cellular immune response [6].

The *tat* gene translates the Tat protein, one of the accessory proteins that strongly activate the viral long terminal repeat (LTR) and essentially induce viral DNA transcription for replication [7]. This protein can interact with the transactivation response (TAR) element and recruit the positive transcription elongation factor b (P-TEFb), which relieves a transcriptional block [8-10]. JDV encodes a Tat protein closely related to the Bovine Immunodeficiency Virus (BIV). Tat, has been shown to powerfully activate the JDV LTR and the LTRs of other lentiviruses, including HIV and BIV [11,12]. Tat can specifically recognize heterologous TAR RNAs using different mechanisms [13].

In addition to the DNA vaccine vectors and target antigens used, the delivery system used for a DNA vaccine is also crucial. Low expression levels of DNA vaccines and the associated weak immune response, especially in animal models, has limited the clinical application of DNA vaccines because it is difficult for vaccines to cross the cell membrane; thus, only a tiny amount of the vaccine may reach an antigen-presenting cell and induce an immune response. Therefore it is necessary to develop an effective DNA vaccine carrier system suitable for animal vaccination [14-16].

Natural and synthetic polymers are the primary choices for non-viral vaccine delivery systems because they are biodegradable, biocompatible, non-toxic, and easy to modify into carriers of genetic material [15,16]. Based on these characteristics, polylactic-co-glycolic acid (PLGA) is considered to have great potential as an effective vaccine delivery agent [17]. PLGA is also known to have a low level of cytotoxicity, and it does not cause an inflammatory response in cells [18]. A PLGA-based delivery system has also been highly recommended due to its good cell uptake characteristic [19].

## MATERIALS AND METHODS

### Consensus implementation for the *tat1* JDV protein and codon optimization

A DNA vaccine model against JDV was constructed based on the consensus sequence derived from the amino acid sequences of the Tat1 protein. Four amino acid sequences from the National Center for Biotechnology Information (NCBI; <https://www.ncbi.nlm.nih.gov/>) were aligned using the MultAlin online software (<http://multalin.toulouse.inra.fr/multalin/>) to generate the consensus sequences. The sequences chosen from NCBI were for JDV Pulukan/2000 (ABV80250); JDV (Q82854); JDV Tabanan/87 (AAA64392); and JDV Kalimantan/2000 (ABV80251). The consensus amino acid sequence was then converted into

nucleotide sequences optimized using codon optimization with the target host *Bos taurus* by Gene Universal Inc. (USA). Also, some unique sequences with lower expression levels were removed using codon optimization [20]. The nucleotide sequences were constructed by adding *Bgl*II and *Eco*RI restriction sites as cloning sites and TAATAA codons as a double-codon stop. The gene was synthesized and cloned to pEGFP-C1 (Clontech, USA) by Gene Universal Inc. (USA).

### Implementation of recombinant DNA cloning and its evaluation

Cloning was carried out by transforming pEGFP-C1-tat (kanamycin resistant) on *Escherichia coli* DH5 $\alpha$  (Research Center of Biotechnology, University Gadjah Mada) by applying the heat shock method. Then, pEGFP-C1-tat was isolated using a maxi plasmid isolation kit (EasyPure HiPure Plasmid MaxiPrep Kit; TransGen Biotech Co., Ltd., China). The isolated pEGFP-C1-tat was evaluated using restriction enzymes (*Eco*RI and *Bgl*II; ThermoFisher Scientific, USA). The polymerase chain reaction (PCR) evaluation was performed using primers EGFP-C: 5'CATGGTCTGCTGGAGTTCGTG3' and SV40\_PA: 5'GAAATTTGTGATGCTATTGC3'.

### Preparation of PLGA-pEGFP-C1-tat and the encapsulated test

The PLGA-pEGFP-C1-tat solution was prepared using the double-emulsion-solvent evaporation (w/o/w) method [21]. A 5% concentration PLGA (lactide:glycolide 50:50; Merck, Germany) solution was prepared by dissolving 0.5 mg of PLGA in 10 mL of dichloromethane (Merck); 4% and 2.5% concentrations of PLGA solution were prepared in the same way. The PLGA solution was used as the oil phase (O) with the recombinant DNA pEGFP-C1-tat as the water phase (W) and the W concentration was adjusted to the concentration of PLGA, namely 0.5%, 1%, and 1.5% (ng/ng). The W DNA recombinant pEGFP-C1-tat was added to 50  $\mu$ L of the O PLGA solution and emulsified using a sonicator for 10 sec to obtain a primary emulsion (W<sub>1</sub>/O). The primary emulsion was added to 200  $\mu$ L of polyvinyl alcohol (PVA; Merck) at a concentration of 1% or 2% and vortexed at 7,500 r/min for 10 sec to obtain a secondary emulsion (W<sub>1</sub>/O/W<sub>2</sub>). The secondary emulsion was then agitated at 200 r/min for 5 h to form pellets. The supernatant was removed and the pellets left at room temperature to evaporate the remaining solvent, then centrifugated at 4,000 r/min for 10 min.

To determine the optimal encapsulated formulation, optimization of the PLGA-DNA-PVA ratio [21] was undertaken (Table 1). The optimal encapsulated formulation was determined by applying the gel inhibition test method [14]. In addition, formulation and preparation of a control delivery system solution using chitosan nanoparticles were carried out using formulation and preparation methods described in a previous study [15].

### Physicochemical characterization analysis of the PLGA-pEGFP-C1-tat complex

The particles formed were characterized by examining their size, size distribution, and the associated zeta potential using a Zetasizer Nano ZS (Malvern Instrument Ltd., UK).

### Stability test with DNase I

The stability test was carried out using DNase I (Rnase-free; New England BioLabs Inc., USA) as described in an existing stability test [22]. One microgram of the PLGA-pEGFP-C1-tat complex or the Chitosan-pEGFP-C1-tat complex was added to 4  $\mu$ L of 10 $\times$  sample buffer and the mixture was incubated with 1  $\mu$ g of DNase I (1 U/mL) at 37°C for 30 min in a water bath. The reaction was stopped by adding 2  $\mu$ L of EDTA (ethylenediaminetetraacetic acid; Merck) followed by incubation for 1 min.

**Table 1.** Formulation arrangements to determine the optimal encapsulation of the PLGA-pEGFP-C1-tat complex

No.	PLGA concentration (% mg/mL)	DNA recombinant/PLGA concentration (% ng/ng)	PVA concentration (% mg/mL)
1	2.5	0.5	1
2	2.5	1	1
3	2.5	1.5	1
4	2.5	0.5	2
5	2.5	1	2
6	2.5	1.5	2
7	4	0.5	1
8	4	1	1
9	4	1.5	1
10	4	0.5	2
11	4	1	2
12	4	1.5	2
13	5	0.5	1
14	5	1	1
15	5	1.5	1
16	5	0.5	2
17	5	1	2
18	5	1.5	2

PLGA, polylactic-co-glycolic acid; PVA, polyvinyl alcohol.

### Nanoparticle cytotoxicity test

Cytotoxicity testing was performed by MTT assays on HeLa cultured cells [15]. HeLa cells were grown on a complex medium consisting of 5 mL of fetal bovine serum (Merck), 1 mL of penicillin-streptomycin (Merck), 250  $\mu$ L Fungizone (Amphotericin B Solution; Merck), in RPMI (StableCell RPMI-1640; Merck) media. Each treatment to be tested was added to 100  $\mu$ L of culture media. For test replication, each sample was tested in a different microplate well. HeLa cells were incubated in a CO<sub>2</sub> incubator for 24 h and then washed with PBS 1 $\times$  (Dulbecco's phosphate buffered saline; Merck) and 100  $\mu$ L of MTT solution (Thiazolyl Blue Tetrazolium Bromide; Merck) at a concentration 0.5 mg/mL was added to each well, including wells containing control media (without cells). The cells were then incubated for 2–4 h in a CO<sub>2</sub> incubator to form formazan crystals. The formazan crystals were then dissolved by adding 100  $\mu$ L of SDS solution to each well, and the microplate was incubated overnight at room temperature. The absorbance of the microplate wells was obtained by using an ELISA Reader at  $\lambda$ 595 nm. The obtained treatment absorbance data were converted into viability percentages.

### Transfection in cultured HeLa cells

Transfection of cultured HeLa cells (Research Center of Biotechnology, University Gadjah Mada) was carried out according to the steps described previously [15,16]. HeLa cells were prepared by culturing the cells in a Petri dish (diameter 60 mm) with a coverslip (diameter 22 mm) in the middle. Cell cultures were incubated at 5% CO<sub>2</sub> and 37°C for 48 h. Transfections with the PLGA-pEGFP-C1-tat or the chitosan-pEGFP-C1-tat complexes were performed. As an additional control, HeLa cultured cells were transfected with EL (TransIntro EL Transfection Reagent; TransGen Biotech Co., Ltd.)-pEGFP-C1-tat and lipofectamine (Lipofectamine 3000 Transfection Reagent; ThermoFisher Scientific)-pEGFP-C1-tat as a commercial control. Cell cultures were exposed to treatment for 4 h. A media was replaced with new culture media every day and incubated for 48 h.

### Fluorescence observation

Observation of fluorescence of the EGFP-tat protein was carried out using a ZEISS LSM 800 confocal fluorescence microscope.

### Total RNA isolation of cultured HeLa cells

Total RNA from cultured HeLa cells was extracted using the *TransZol* Up Plus RNA Kit (TransGen Biotech Co., Ltd.), following the protocol in the kit's manual.

### Synthesis of cDNA from total RNA isolation and PCR

Synthesis of cDNA from total RNA isolation of culture HeLa cells was carried out using a High-Capacity cDNA Reverse Transcription Kit (ThermoFisher Scientific) following the method included in the kit's manual. PCR was performed using the forward primer for the EGFP-C region (5'CATGGTCCTGCTGGAGTTCGTG3') and the reverse primer for the tat region (5'TGCCCTCTTCTTTCTCCTT3').

### Real-time PCR

The synthetic DNA stock used previously for transformation was used as a positive control. The internal control for the real-time PCR was glyceraldehyde 3-phosphate dehydrogenase (GAPDH). The forward primer was 5'GAAGGTGAAGGTCGGAGTC3' and the reverse primer was 5'GAAGATGGTGATGGGATTC3' [15,16].

## RESULTS

### JDV tat gene construction

Four amino acid sequences from NCBI were aligned using the MultAlign program to generate consensus sequences (Fig. 1A). The amino acid consensus sequence was converted into a nucleotide sequence for codon optimization without changing the amino acid sequence (Fig. 1B). The transgene was chemically synthesized with *Bgl*II and *Eco*RI restriction sites and cloned into the pEGFP-C1 vector (pEGFP-C1-tat).

### Recombinant DNA cloning and evaluation

The transformation succeeded in producing transformant bacteria (Supplementary Fig. 1). Evaluation of the restriction enzyme showed two bands of size 4,711 bp and 303 bp (Fig. 2). Also, the results of the evaluation by the PCR method produced a clear band with a 593 bp size (Fig. 3).

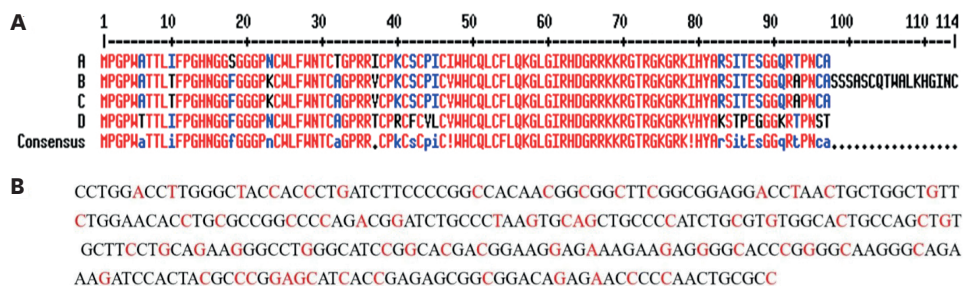
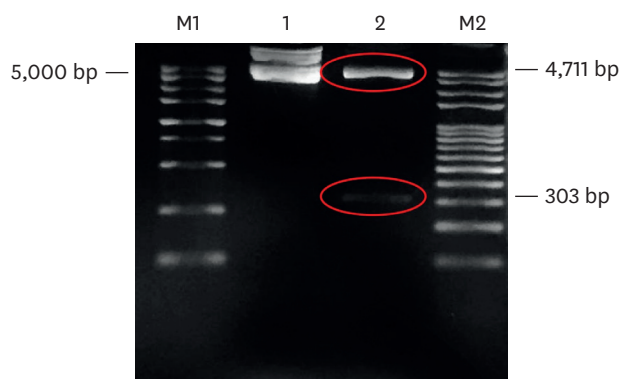
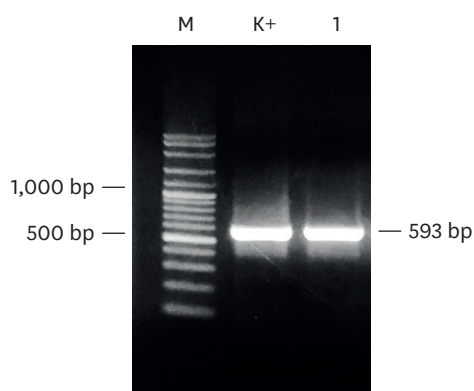


Fig. 1. JDV tat gene construction on the pEGFP-C1 vector. (A) Consensus of four amino acid sequences of the tat1 protein of JDV. (B) Optimized sequence of JDV tat with red characters showing the substituted nucleotide for codon optimization. JDV, Jembrana disease virus



**Fig. 2.** Visualization of evaluation results using restriction enzymes on isolated recombinant DNA (pEGFP-C1-tat) from transformant bacteria.

M1, marker 5,000 bp; M2, marker 100 bp; 1, without evaluation with restriction enzymes (negative control); 2, with evaluation using the restriction enzyme *Bgl*III and *Eco*RI.



**Fig. 3.** Results of amplification of the *tat* gene by PCR.

PCR, polymerase chain reaction; M, marker 100 bp; K+, stock of pEGFP-C1-tat recombinant DNA used for transformation; 1, isolated recombinant DNA (pEGFP-C1-tat) from transformant bacteria.

### Encapsulated analysis of the PLGA-pEGFP-C1-tat complex from the formulation

The results of the PLGA-pEGFP-C1-tat complex analysis showed that the encapsulation efficiency of pEGFP-C1-tat increased with an increase in the concentrations of the PLGA and PVA (Fig. 4). The PLGA:DNA:PVA ratio used for further analysis was 4%:0.5%:2%, which was based on the efficiency of the material.

### Physicochemical characterization analysis of the PLGA-pEGFP-C1-tat complex

The physicochemical characterization results showed that the PLGA-pEGFP-C1-tat complex has a polydispersity index of 0.246, a size of 943.4 nm (Fig. 5A), and a zeta potential of -2.31 mV (Fig. 5B).

### Stability test with DNase I

The stability test results showed that complex could protect pEGFP-C1-tat from the degradation by DNase I, whereas the pEGFP-C1-tat without PLGA or chitosan was degraded by DNase I (Fig. 6).

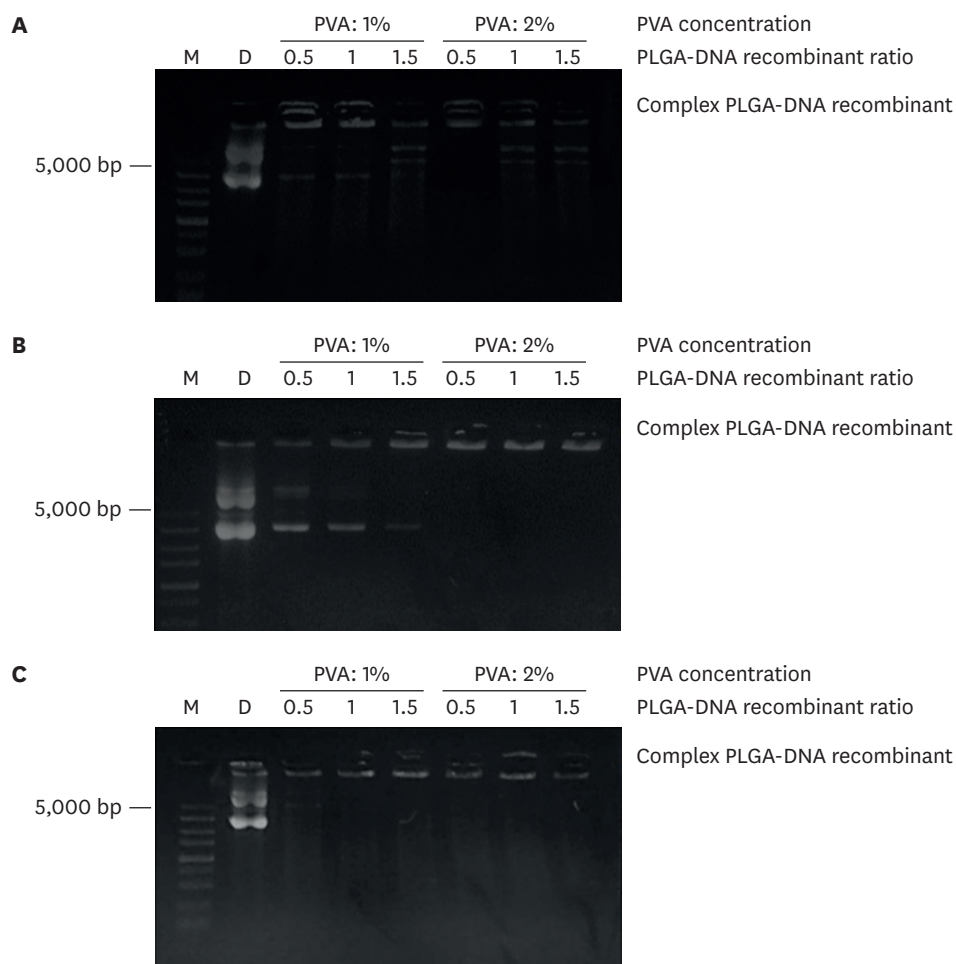


**Fig. 4.** Visualization of the PLGA-pEGFP-C1-tat complex. (A) 2.5% PLGA concentration. (B) 4% PLGA concentration. (C) 5% PLGA concentration. PLGA, polylactic-co-glycolic acid; PVA, polyvinyl alcohol.

### Cytotoxicity test of the PLGA-pEGFP-C1-tat complex

Based on the cytotoxic test results, the percentage of living cells was 98.03% when using PLGA-pEGFP-C1-tat (**Fig. 7**).

### Observation of the EGFP-tat fusion protein

The results showed the presence of green luminescence in both the PLGA-pEGFP-C1-tat (**Fig. 8G**) and Chitosan-pEGFP-C1-tat (**Fig. 8H**) delivery systems, whereas the negative controls did not produce any green luminescence (**Fig. 8B-F**). However, luminescence was seen in the positive control, namely pEGFP-C1-tat transfected with the commercial transfection reagents (**Fig. 8I and J**).

### pEGFP-C1-tat mRNA expression analysis

The total RNA concentrations ranged from 423.78–457.64 ng/ $\mu$ L. The two-step reverse transcriptase PCR electrophoresis using chitosan-pEGFP-C1-tat and PLGA-pEGFP-C1-tat revealed a single band of 296 bp (**Fig. 9**). Melting curve analysis shows a single peak with a  $T_m$  of 89.5°C (**Fig. 10**). Based on the mean fold change value obtained, the PLGA-pEGFP-C1-tat treatment produced a 1.74-fold change, while the chitosan-pEGFP-C1-tat fold change was 2.06 (**Fig. 11**).

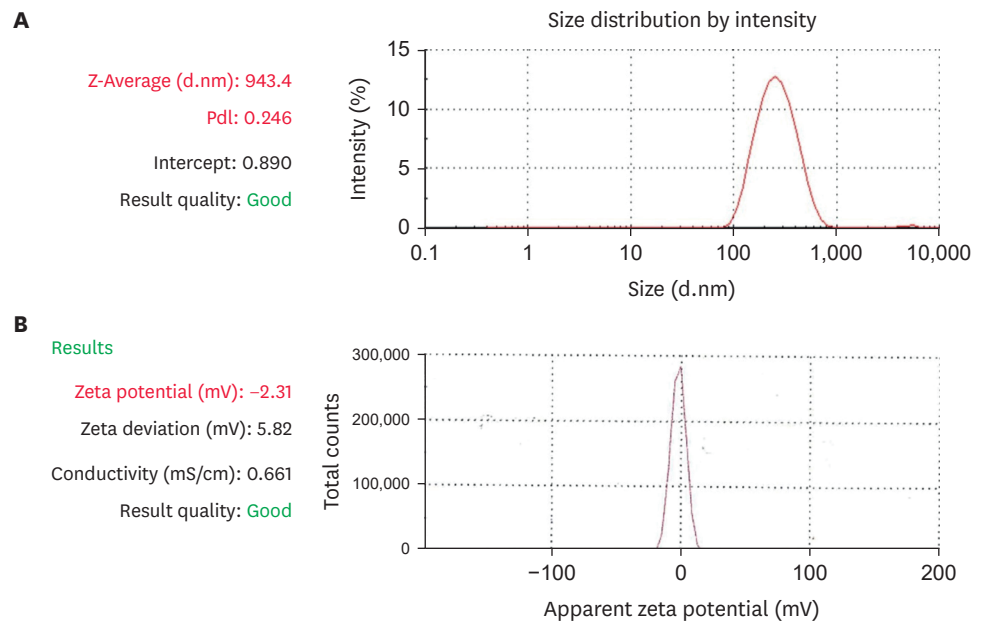


**Fig. 5.** Physicochemical characterization of the PLGA-pEGFP-C1-tat complex. (A) Results of measuring the size and distribution of particles from the PLGA-pEGFP-C1-tat complex. (B) Results of zeta potential measurement of the PLGA-pEGFP-C1-tat complex.

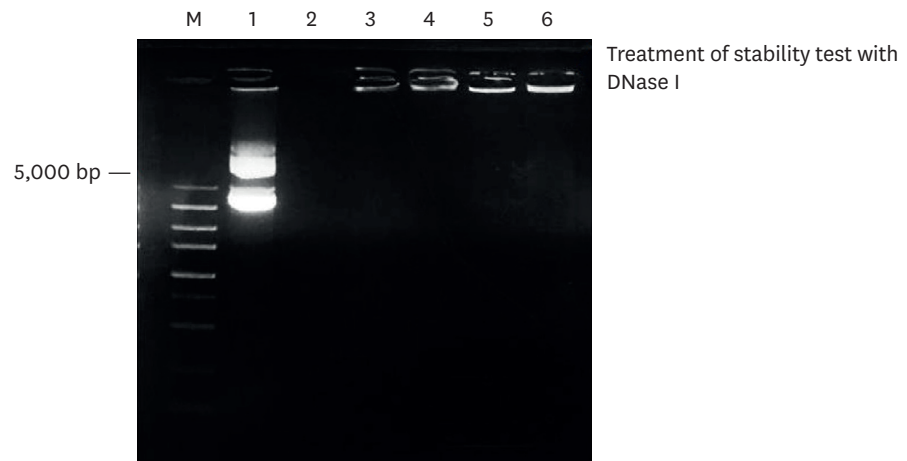


**Fig. 6.** Complex stability test of PLGA-pEGFP-C1-tat. M, DNA marker 5,000 bp; 1, recombinant DNA without adding DNase I; 2, recombinant DNA with addition of DNase I; 3, PLGA-pEGFP-C1-tat complex without adding DNase I; 4, PLGA-pEGFP-C1-tat complex with addition of DNase I; 5, chitosan-pEGFP-C1-tat complex without the addition of DNase I; 6, chitosan-pEGFP-C1-tat complex with addition of DNase I.

## DISCUSSION

This study designed a novel vaccine based on consensus amino acid sequences, an approach that was previously implemented in the development of a vaccine against rabies virus [23], avian influenza [24], and hepatitis B [25]. The consensus approach was based on the hypothesis that the respective consensus amino acid is more stable than non-conserved amino acids at a given position [26]. The consensus design approach has had a high impact on functional and non-functional proteins [27].



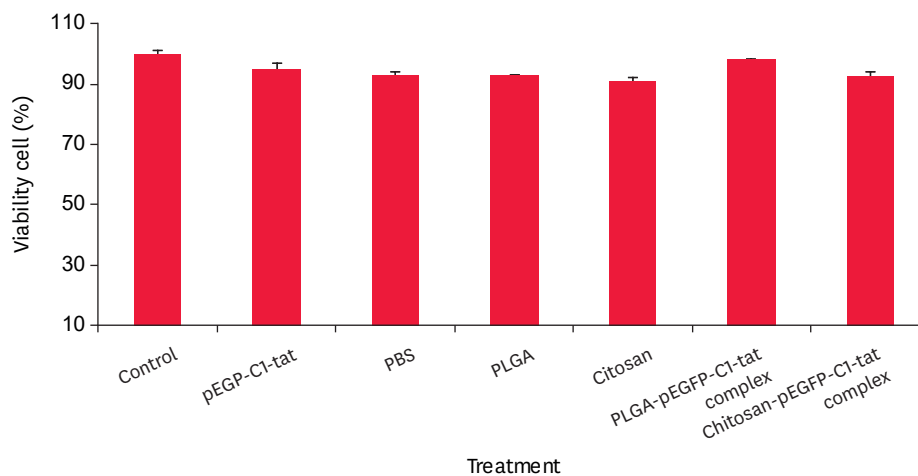


**Fig. 7.** Relative cell viability to PLGA-pEGFP-C1-tat complex. PBS, phosphate buffered saline; PLGA, polylactic-co-glycolic acid.

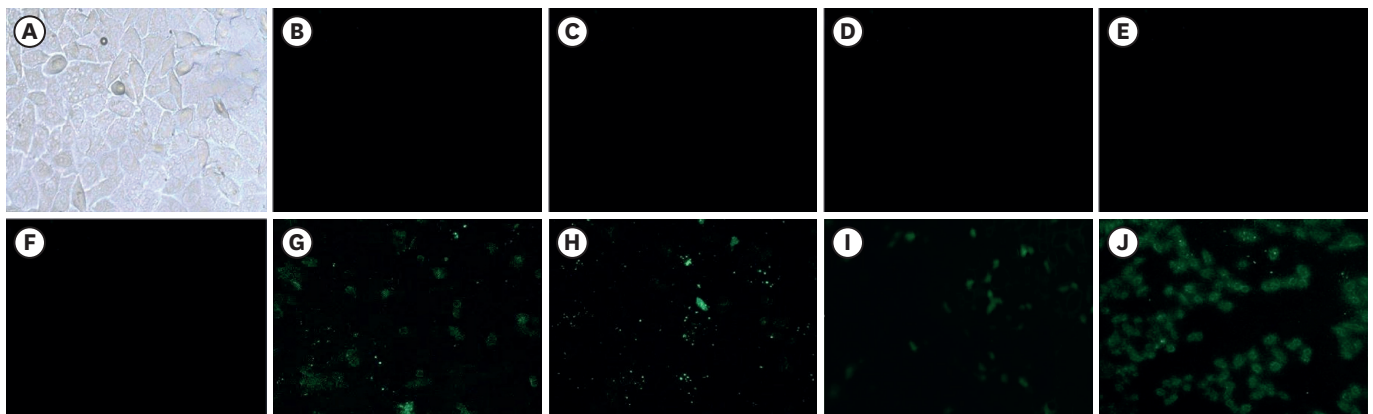


**Fig. 8.** Fluorescence observation of EGFP-tat fusion protein in HeLa cells. (A) Cultured HeLa cells. (B) Cultured HeLa cells without transfection (negative control). (C) Cultured HeLa cells were transfected using PBS (negative control). (D) Cultured HeLa cells were transfected using PLGA without pEGFP-C1-tat (negative control). (E) Cultured HeLa cells were transfected using chitosan without pEGFP-C1-tat (negative control). (F) Cultured HeLa cells were transfected using pEGFP-C1-tat without a delivery system (negative control). (G) Cultured HeLa cells transfected using the PLGA-pEGFP-C1-tat complex. (H) Cultured HeLa cells transfected using the chitosan-pEGFP-C1-tat complex (comparison control). (I) Cultured HeLa cells transfected using the EL-pEGFP-C1-tat complex (commercial control). (J) Cultured HeLa cells transfected using the lipofectamine-pEGFP-C1-tat complex (commercial control). PBS, phosphate buffered saline.

The second step in designing the DNA vaccine model involved the construction of a codon-optimized nucleotide sequence that encodes the Tat consensus antigen. The codon optimization of this gene sequence was similar to that used to increase the expression of the Lentivirus gene in a eukaryotic host [28]. Additionally, exclusion of some motif sequences has been suggested to avoid low plasmid production in host cloning or low translation of target protein in the host expression [20].

To further confirm the creation of pEGFP-C1-tat, isolation was undertaken with restriction enzymes. The pEGFP-C1-tat, if cut with two appropriate restriction enzymes (*Bgl*II and *Eco*RI) it produces two DNA strands: the vector backbone (4,711 bp) and the gene insert (303 bp). The pEGFP-C1-tat was also assessed by applying the PCR method. The EGFP-C primer attaches to the ORF EGFP region, while the SV40\_PA primer attaches to a downstream

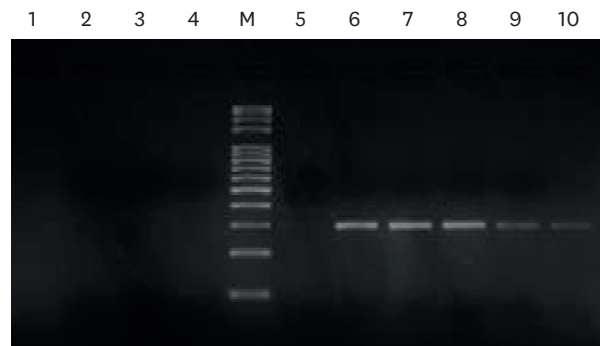


**Fig. 9.** PCR product visualization. PCR, polymerase chain reaction; PBS, phosphate buffered saline; PLGA, polylactic-co-glycolic acid; 1, cultured HeLa cells without transfection (negative control); 2, cultured HeLa cells transfected using PBS (negative control); 3, cultured HeLa cells transfected using PLGA without pEGFP-C1-tat (negative control); 4, cultured HeLa cells transfected using chitosan without pEGFP-C1-tat (negative control); M, DNA marker 100 bp; 5, cultured HeLa cells transfected using pEGFP-C1-tat without a delivery system (negative control); 6, synthetic pEGFP-C1-tat stock previously used for transformation; 7, cultured HeLa cells transfected using the Lipofectamine-pEGFP-C1-tat complex (commercial control); 8, cultured HeLa cells transfected using the EL-pEGFP-C1-tat complex (commercial control); 9, cultured HeLa cells transfected using the Chitosan-pEGFP-C1-tat complex (comparison control); 10, cultured HeLa cells transfected using the PLGA-pEGFP-C1-tat complex.

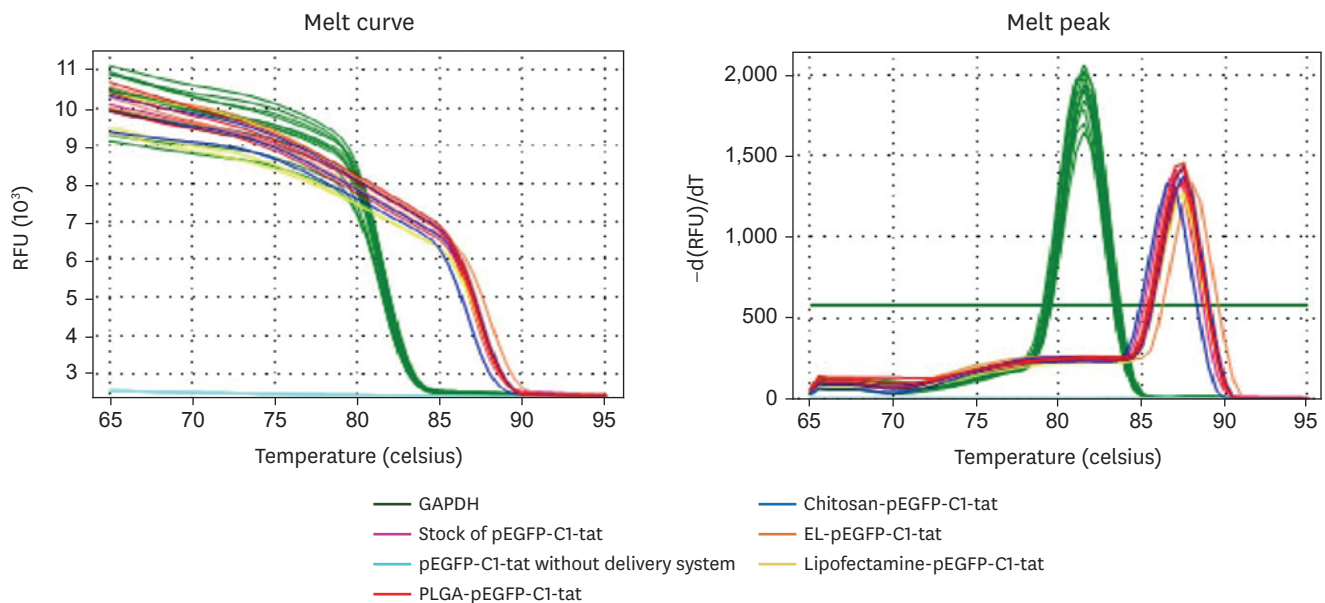


**Fig. 10.** Melting curve (A) and melting peak (B) profiles.

region, and the estimated PCR product is 593 bp. PCR product sizes are larger than the target gene due to the increase of several pairs of bases that belong to EGFP and SV40\_PA regions.

The electrophoresis results of the PLGA-pEGFP-C1-tat complex in this study indicated that the encapsulated efficiency of PLGA to the recombinant DNA pEGFP-C1-tat was relatively high and increased with increasing concentrations of PLGA and PVA. Moreover, the recombinant DNA without PLGA and chitosan could migrate freely during electrophoresis. However, with increasing concentrations of PLGA and PVA used, the recombinant DNA becomes entangled and encapsulated, remaining in the gel well and not migrating during electrophoresis. Encapsulation efficiency was significantly increased by increasing the concentration of PLGA [29]. This phenomenon is likely the result of the increased viscosity of the multiple emulsions. An increase in viscosity can prevent the diffusion of DNA out of the oil phase so that the DNA will remain encapsulated in the PLGA matrix [29].

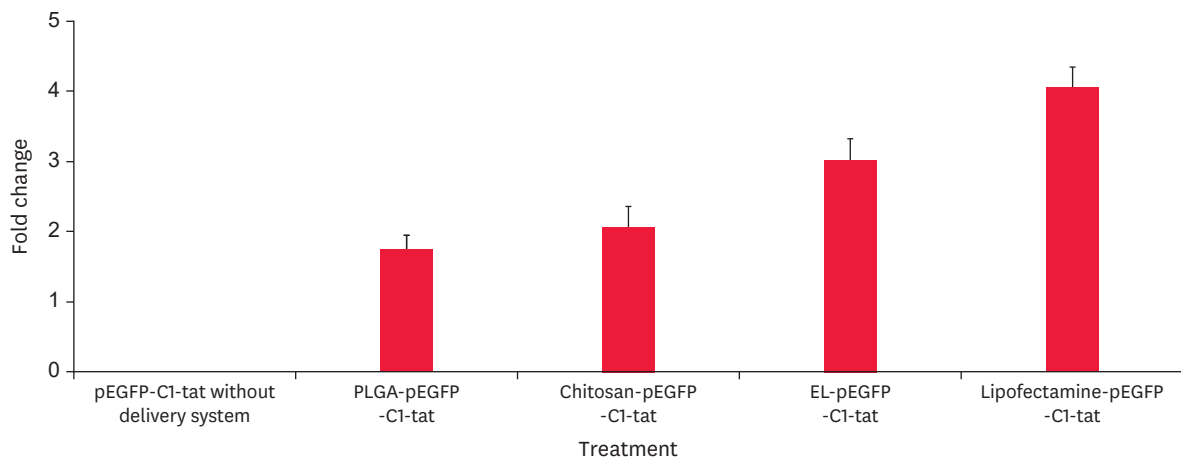


Fig. 11. Relative expressions of pEGFP-C1-tat mRNA using various delivery systems.

Nanoparticle size determines the ease with which these particles enter the cell; the smaller the particle size, the easier it is to enter the cell, and absorption will increase [30].

The size distribution analysis results show that the PLGA-pEGFP-C1-tat complex has a monodisperse size distribution with a polydispersity index value of 0.246. Polydispersity index values close to 0 indicate a homogeneous particle size dispersion. The smaller the polydispersity index, the more similar the particle sizes; this is important because a large size difference will affect the characteristics of the particles [31]. In addition, a low polydispersity index indicates that the dispersion is likely to be more stable over the long term [32]. Meanwhile, the particle size of the PLGA-DNA recombinant complex in this study was similar to the particle size of the PLGA-DNA recombinant complex described by other researchers, namely 884 nm [33].

The characteristics of the surface charge properties of the PLGA-pEGFP-C1-tat complex need to be determined to indicate the stability of the colloid system. Such stability is indicated by the zeta potential value or the surface charge properties of the particles. A high zeta potential can prevent the aggregation process on the particles due to the repulsion and stabilization of the particle dispersion. The zeta potential measurement of the PLGA-pEGFP-C1-tat complex was  $-2.31$  mV. The negative charge on the surface of the particles was due to the negatively charged carboxyl groups of PLGA and the ionization of the acetate groups present in PVA [34]. PVA is required during the formation of the PLGA-DNA recombinant complex as it acts as a particle stabilizer to increase the efficiency of recombinant DNA encapsulation [33]. A similar zeta potential value ( $-3.3$  mV) was obtained by other researchers [35]. This negative charge is a characteristic of a PLGA delivery system; this causes PLGA to have low cytotoxicity as the negative charge does not damage the integrity of the plasma membrane and does not damage mitochondria or lysosomes compared to that caused by a positively charged particle complex [19]. Although the charge of the PLGA-pEGFP-C1-tat complex is negative, the complex still had a good cell uptake value because a PLGA delivery system is mediated by clathrin-independent endocytosis to pass through the cell membrane [36].

Based on the stability test results using DNase I, it was shown that no recombinant DNA was degraded. These results indicate that PLGA associates with the pEGFP-C1-tat effectively [37]. Furthermore, pEGFP-C1-tat in line 1 is circular DNA and, its isolation process which using

chemical techniques causes several conformations to form different bands. Free plasmid DNA can migrate into several DNA bands that show several different plasmid conformations [15,16], while in lines 3–6 with the PLGA and chitosan delivery system formulations will make the DNA unable to migrate because the DNA is trapped in the delivery system and cannot pass through the pores of the agarose gel [15,16]. In this case, the delivery system can also protect DNA from degradation by the DNase I enzyme, this can be evidence of the stability of the formulation which can be seen in lines 4 and 6.

The cytotoxicity test results showed that the PLGA delivery system is non-toxic and considered to provide a high level of security for the cell. The low cytotoxic effect of the PLGA delivery system for the recombinant DNA is because PLGA is composed of endogenous original monomers lactic and glycolic acids, which are quickly metabolized in the body through the Krebs cycle resulting in its systemic cytotoxic effects to be minimal and considered safe [38]. Also, the negative charge in the PLGA delivery system does not damage the integrity of the cell membrane at the time of endocytosis, does not cause damage to cell lysosomes [19], and does not cause an inflammatory response [18].

The detection of luminescence in HeLa cells transfected with the PLGA and chitosan delivery systems showed that the EGFP-tat fusion gene was successfully expressed. The luminescence produced by the cells also shows that chitosan nanoparticles and PLGA have a role in delivering plasmids to the cell nucleus [15,16].

The presence of DNA bands visualized on agarose gel on pEGFP-C1-tat mRNA expression analysis showed that the pEGFP-C1-tat chitosan and PLGA delivery systems can produce the desired mRNA. It also showed that the PLGA delivery system can successfully express pEGFP-C1-tat mediated by clathrin-independent endocytosis to cross the cell membrane of target cells [36].

In confirming the amplification product was similar to the target product, the synthetic pEGFP-C1-tat stock previously used for transformation was used as a positive control in assessing the melting curve profile with real-time PCR. Melting curve profile in real-time PCR is needed to ensure the PCR target band matches the target band in the initial product and confirms the specificity of the primer used [15,16]. The single peak observed in the melting curve shows that the primer is suitable, and there has been no decrease or increase in the number of nucleotide bases.

Based on the results of pEGFP-C1-tat mRNA expression analysis using real-time PCR, it can be seen that a PLGA delivery system can deliver pEGFP-C1-tat into cells and is expressed as mRNA in the form of an EGFP-tat fusion, whereas the naked pEGFP-C1-tat without the delivery system does not produce a fold change value. The chitosan-pEGFP-C1-tat resulted in a higher expression level than the PLGA-pEGFP-C1-tat. This is due to the positive charge of the chitosan-pEGFP-C1-tat, making it easier for nanoparticles to bind to cell membranes and facilitating intracellular mobility of nanoparticles in the cytoplasmic compartment [15,16].

In conclusion, the negative charge formed by the PLGA-pEGFP-C1-tat complex is advantageous because a negatively charged delivery complex causes minimal damage to target cells; thus, PLGA is effective as a delivery system for drugs and therapies over the long term [19]. Based on the results of this study, PLGA has good potential as a delivery system for pEGFP-C1-tat.

## SUPPLEMENTARY MATERIAL

### Supplementary Fig. 1

Culture on agar media containing the antibiotic kanamycin. (A) *Escherichia coli* DH5 $\alpha$  bacteria that were not transformed with pEGFP-C1-tat (negative control). (B) *E. coli* DH5 $\alpha$  bacteria were transformed with pEGFP-C1-tat (transformant bacteria).

[Click here to view](#)

## REFERENCES

1. Tanaya IWM. Bio-molecular study of Jembrana virus: as basic development of tissue culture vaccine. *Bul Vet Udayana*. 2016;8(2):187-202.
2. Kusumawati A, Wanahari A, Astuti P, Kurniasih, Mappakaya BA, Wuryastuty H. Vaccine against Jembrana disease virus infection: a summary findings. *Am J Immunol*. 2015;11(3):68-73.  
[CROSSREF](#)
3. Kusumawati A, Wanahari TA, Putri RF, Untari T, Hartati S, Mappakaya BA, et al. Clinical and pathological perspectives of Jembrana disease virus infection: a review. *Biosci Biotechnol Res Asia*. 2014;11(3):1221-1225.  
[CROSSREF](#)
4. Suwiti NK. The phenomenon Jembrana disease and bovine immunodeficiency viruses in Bali cattle. *Bul Vet Udayana*. 2009;1(1):21-25.
5. Agustini NLP, Masa Tenaya IW, Supartika IK. Effication test of Jembrana disease vaccine. *Bul Vet*. 2009;27(86):1-16.
6. Xu K, Ling ZY, Sun L, Xu Y, Bian C, He Y, et al. Broad humoral and cellular immunity elicited by a bivalent DNA vaccine encoding HA and NP genes from an H5N1 virus. *Viral Immunol*. 2011;24(1):45-56.  
[PUBMED](#) | [CROSSREF](#)
7. Chen H, Wilcox G, Kertayadnya G, Wood C. Characterization of the Jembrana disease virus tat gene and the cis- and trans-regulatory elements in its long terminal repeats. *J Virol*. 1999;73(1):658-666.  
[PUBMED](#) | [CROSSREF](#)
8. Mancebo HS, Lee G, Flygare J, Tomassini J, Luu P, Zhu Y, et al. P-TEFb kinase is required for HIV Tat transcriptional activation *in vivo* and *in vitro*. *Genes Dev*. 1997;11(20):2633-2644.  
[PUBMED](#) | [CROSSREF](#)
9. Marshall NF, Peng J, Xie Z, Price DH. Control of RNA polymerase II elongation potential by a novel carboxyl-terminal domain kinase. *J Biol Chem*. 1996;271(43):27176-27183.  
[PUBMED](#) | [CROSSREF](#)
10. Zhu Y, Pe'ery T, Peng J, Ramanathan Y, Marshall N, Marshall T, et al. Transcription elongation factor P-TEFb is required for HIV-1 tat transactivation *in vitro*. *Genes Dev*. 1997;11(20):2622-2632.  
[PUBMED](#) | [CROSSREF](#)
11. Cheng-Mayer C, Shioda T, Levy JA. Host range, replicative, and cytopathic properties of human immunodeficiency virus type 1 are determined by very few amino acid changes in tat and gp120. *J Virol*. 1991;65(12):6931-6941.  
[PUBMED](#) | [CROSSREF](#)
12. Chen H, He J, Fong S, Wilcox G, Wood C. Jembrana disease virus Tat can regulate human immunodeficiency virus (HIV) long terminal repeat-directed gene expression and can substitute for HIV Tat in viral replication. *J Virol*. 2000;74(6):2703-2713.  
[PUBMED](#) | [CROSSREF](#)
13. Smith CA, Calabro V, Frankel AD. An RNA-binding chameleon. *Mol Cell*. 2000;6(5):1067-1076.  
[PUBMED](#) | [CROSSREF](#)
14. Boyoglu S, Vig K, Pillai S, Rangari V, Dennis VA, Khazi F, et al. Enhanced delivery and expression of a nanoencapsulated DNA vaccine vector for respiratory syncytial virus. *Nanomedicine*. 2009;5(4):463-472.  
[PUBMED](#) | [CROSSREF](#)
15. Unsunnidhal L, Ishak J, Kusumawati A. Expression of *gag*-CA gene of Jembrana disease virus with cationic liposomes and chitosan nanoparticle delivery systems as DNA vaccine candidates. *Trop Life Sci Res*. 2019;30(3):15-36.  
[CROSSREF](#)

16. Ishak J, Unsunnidhal L, Martien R, Kusumawati A. *In vitro* evaluation of chitosan-DNA plasmid complex encoding Jembrana disease virus env-tm protein as a vaccine candidate. *J Vet Res (Pulawy)*. 2019;63(1):7-16.  
[PUBMED](#) | [CROSSREF](#)
17. Zhao K, Li W, Huang T, Luo X, Chen G, Zhang Y, et al. Preparation and efficacy of Newcastle disease virus DNA vaccine encapsulated in PLGA nanoparticles. *PLoS One*. 2013;8(12):e82648.  
[PUBMED](#) | [CROSSREF](#)
18. Mura S, Hillaireau H, Nicolas J, Le Droumaguet B, Gueutin C, Zanna S, et al. Influence of surface charge on the potential toxicity of PLGA nanoparticles towards Calu-3 cells. *Int J Nanomedicine*. 2011;6:2591-2605.  
[PUBMED](#) | [CROSSREF](#)
19. Fröhlich E. The role of surface charge in cellular uptake and cytotoxicity of medical nanoparticles. *Int J Nanomedicine*. 2012;7:5577-5591.  
[PUBMED](#) | [CROSSREF](#)
20. Williams JA. Vector design for improved DNA vaccine efficacy, safety and production. *Vaccines (Basel)*. 2013;1(3):225-249.  
[PUBMED](#) | [CROSSREF](#)
21. Zhao K, Zhang Y, Zhang X, Shi C, Wang X, Wang X, et al. Chitosan-coated poly(lactic-co-glycolic) acid nanoparticles as an efficient delivery system for Newcastle disease virus DNA vaccine. *Int J Nanomedicine*. 2014;9:4609-4619.  
[PUBMED](#) | [CROSSREF](#)
22. Huang T, Song X, Jing J, Zhao K, Shen Y, Zhang X, et al. Chitosan-DNA nanoparticles enhanced the immunogenicity of multivalent DNA vaccination on mice against *Trueperella pyogenes* infection. *J Nanobiotechnology*. 2018;16(1):8.  
[PUBMED](#) | [CROSSREF](#)
23. Starodubova S, Kuzmenko YV, Latanova AA, Preobrazhenskaya OV, Karpov VL. Creation of DNA vaccine vector based on codon-optimized gene of rabies virus glycoprotein (G protein) with consensus amino acid sequence. *Mol Biol*. 2016;50(2):328-331.  
[CROSSREF](#)
24. Laddy DJ, Yan J, Corbitt N, Kobinger GP, Weiner DB. Immunogenicity of novel consensus-based DNA vaccines against avian influenza. *Vaccine*. 2007;25(16):2984-2989.  
[PUBMED](#) | [CROSSREF](#)
25. Obeng-Adjei N, Yan J, Choo D, Weiner D. Immunogenicity of novel consensus-based DNA vaccines against hepatitis B core antigen. *J Immunol*. 2011;186(1 Suppl):106.1.
26. Porebski BT, Buckle AM. Consensus protein design. *Protein Eng Des Sel*. 2016;29(7):245-251.  
[PUBMED](#) | [CROSSREF](#)
27. Porebski BT, Nickson AA, Hoke DE, Hunter MR, Zhu L, McGowan S, et al. Structural and dynamic properties that govern the stability of an engineered fibronectin type III domain. *Protein Eng Des Sel*. 2015;28(3):67-78.  
[PUBMED](#) | [CROSSREF](#)
28. Haas J, Park EC, Seed B. Codon usage limitation in the expression of HIV-1 envelope glycoprotein. *Curr Biol*. 1996;6(3):315-324.  
[PUBMED](#) | [CROSSREF](#)
29. Zhao K, Li GX, Jin YY, Wei HX, Sun QS, Huang TT, et al. Preparation and immunological effectiveness of a Swine influenza DNA vaccine encapsulated in PLGA microspheres. *J Microencapsul*. 2010;27(2):178-186.  
[PUBMED](#) | [CROSSREF](#)
30. Mohanraj VJ, Chen Y. Nanoparticles - a review. *Trop J Pharm Res*. 2006;5(1):561-573.  
[CROSSREF](#)
31. Avadi MR, Sadeghi AM, Mohammadpour N, Abedin S, Atyabi F, Dinarvand R, et al. Preparation and characterization of insulin nanoparticles using chitosan and Arabic gum with ionic gelation method. *Nanomedicine (Lond)*. 2010;6(1):58-63.  
[PUBMED](#) | [CROSSREF](#)
32. Gao L, Zhang D, Chen M. Drug nanocrystals for the formulation of poorly soluble drugs and its application as a potential drug delivery system. *J. Nanopart*. 2008;10(5):845-862.  
[CROSSREF](#)
33. Ravi Kumar MN, Bakowsky U, Lehr CM. Preparation and characterization of cationic PLGA nanospheres as DNA carriers. *Biomaterials*. 2004;25(10):1771-1777.  
[PUBMED](#) | [CROSSREF](#)
34. Lúcio M, Carvalho A, Lopes I, Gonçalves O, Bárbara E, Oliveira M. Polymeric versus lipid nanoparticles: comparative study of nanoparticulate systems as indomethacin carriers. *J Appl Solut Chem Model*. 2015;4(2):95-109.  
[CROSSREF](#)

35. Amir Kalvanagh P, Ebtokara M, Kokhaei P, Soleimanjahi H. Preparation and characterization of PLGA nanoparticles containing plasmid DNA encoding human IFN-lambda-1/IL-29. *Iran J Pharm Res.* 2019;18(1):156-167.  
[PUBMED](#)
36. Palocci C, Valletta A, Chronopoulou L, Donati L, Bramosanti M, Brasili E, et al. Endocytic pathways involved in PLGA nanoparticle uptake by grapevine cells and role of cell wall and membrane in size selection. *Plant Cell Rep.* 2017;36(12):1917-1928.  
[PUBMED](#) | [CROSSREF](#)
37. Xu Q, Crossley A, Czernuszka J. Preparation and characterization of negatively charged poly(lactic-co-glycolic acid) microspheres. *J Pharm Sci.* 2009;98(7):2377-2389.  
[PUBMED](#) | [CROSSREF](#)
38. Danhier F, Ansorena E, Silva JM, Coco R, Le Breton A, Pr at V. PLGA-based nanoparticles: an overview of biomedical applications. *J Control Release.* 2012;161(2):505-522.  
[PUBMED](#) | [CROSSREF](#)